Experimental and numerical study of residual stress evolution in cold spray coating

R. Ghelichi [a,b,*], S. Bagherifard [a,b], D. MacDonald [c], I. Fernandez-Pariente [d], B. Jodoin [c], M. Guagliano [a]

[a] Politecnico di Milano, Via G. la Masa, 1, 20156 Milan, Italy
[b] Massachusetts Institute of Technology, 77 Massachusetts Avenue, Cambridge, MA 02139-4307, United States
[c] University of Ottawa, 770 King Edward, Ottawa, ON, Canada K1N 6N5
[d] University of Oviedo, Department of Materials and Metallurgy Engineering, Campus de Viesques, 33203 Gijón, Spain

Article history:
Received 30 July 2013
Received in revised form
11 September 2013
Accepted 12 September 2013
Available online 3 October 2013

1. Introduction

Residual stresses are present in materials that are produced by nearly every mechanical, chemical, and thermal process, including coatings [1]. As a result, most metallic and ceramic coatings are in a state of internal residual stress. The residual stress can be either compressive or tensile. It is generally recognized that compressive stresses in coatings are more favorable due to their positive effect on the fatigue life and strength of the materials, components and structures [1,2]. A number of factors influence the residual stress level in thermal spray coatings, including quenching the sprayed material due to high cooling rate, peening effect due to the plastic deformation of non-molten or semi-molten particles impacting the substrate, thermal mismatch between the coating and substrate materials and temperature gradient in multi-pass deposition processes. Constant bombardment of particles on the substrate and coating area is known as a major feature that results in increasing the residual stresses [3]. Cold spray process, is principally different from other types of thermal spray coating process, in terms of its lower process temperature and higher particle impact velocity, both of which affect directly the resulting residual stress distribution. Experimental studies have been performed on residual stresses distribution generated during the cold spray coating process and similar impact based processes. McCune et al. [4] have measured residual stresses for copper coatings and Bagherifard et al. [5] performed X-ray diffraction (XRD) measurements on stresses induced in aluminum coatings. Ghelichi et al. [2] measured the residual stress of different Al alloy coated samples and studied their effect on fatigue behavior. An interesting common observation in almost all studies is the relaxation of the compressive residual stresses at the interface of the coating and the substrate; conversely, the major difference is the reported stress in the substrate that is almost zero in [4] whereas considerable values with respect to that of the deposited material are observed in other studies [2,5]. There are very few studies which follow empirical approaches for residual stress measurement in cold spray coated samples. Luzin et al. [6] studied the residual stress in Cu and Al coated samples by neutron powder diffraction stress measurement. They used the Tsui and Clyne's progressive model [7] that is

* Corresponding author. Tel.: +39 0223998206.
E-mail addresses: ghelichi@mit.edu (R. Ghelichi), sbagheri@mit.edu (S. Bagherifard), daniel.macdonald@uottawa.ca (D. MacDonald), inesfp@uniovi.es (I. Fernandez-Pariente), Bertrand.Jodoin@uottawa.ca (B. Jodoin), mario.guagliano@polimi.it (M. Guagliano).

Nomenclature

D	diameter
D_{rr}, Q	Rosin–Rammler distribution parameters
V	velocity
ρ	density
M	Mach number
A	area
T	temperature
μ	viscosity
Pr	Prandtl number
Re	Reynolds number
C_p	heat capacity
B_1, B_2, n, C, m	Johnson-Cook material model constants
$\in_p (\in_{p0})$	equivalent plastic strain
$\dot{\in}_p (\dot{\in}_{p0})$	equivalent plastic strain rate
$T\,(T_{init})$	temperature
T_{melt}	melting temperature
σ_{eq}	equivalent normal plastic stress
t	time
S, S_1	Zenner-Wer-Avrami constants
K	Boltzman constant
ΔH	activation enthalpy for the relaxation process

Suffixes

*	throat
e	exit of the nozzle
0	initial condition
a	annealing
C_D	drag coefficient

originally developed to model the residual stress accumulation in thermal spray coatings, to interpret the results empirically. Luzin et al. [6] concluded that the residual stress is determined almost entirely by the plastic deformation process of the spray material due to the high velocity impact of the particles and that the thermal effects do not play a notable role in changing the distribution of the induced stresses. The Tsui and Clyne's approach [7] considers the effect of temperature as a parameter to introduce the residual stress due to the mismatch of the thermal expansions.

Spencer et al. [8] also followed the same approach using Tsui and Clyne's progressive model [7] to interpret the residual stress distribution obtained by using neutron diffraction with high spatial resolution on Al and Al alloy cold spray coatings deposited on Mg substrates. They concluded that the residual stress profiles depend more on the alloy content, i.e. intrinsic resistance to plastic deformation, than on the spray processing conditions. However, they also reported that in cases where the spray temperature was high, the thermal mismatch effect was more notable and affected the obtained residual stress profile [8]. It is to be mentioned that Tsui and Clyne's model [7] considers the effect of temperature as the main reason of curvature change due to the thermal mismatch; whereas the annealing effect of the temperature has not been taken into account.

In fact, one peculiar factor in the cold spray coating process with respect to other impact based peening treatments, such as shot peening, is the gas temperature; the bombardment of the particles induces residual stress in the substrate while the gas temperature can have a simultaneous annealing effect on the residual stress induced by those impacts. Thus, the favorable compressive residual stress induced intrinsically by the continuous peening of the surface can be partially relieved by the process temperature itself. Although the previous studies show the importance of the temperature in the coated samples [9], it is assumed that this parameter can have a negative side effect in this regard.

Previous study of the authors revealed notable difference in residual stress distribution for samples of the same substrate coated with different powders [2]. It was postulated that rather than other parameters, the gas temperature that is adopted for each powder type can play an in situ annealing role and consequently partially relax the residual stresses induced by the high velocity impacts. To the best of authors' knowledge, the conflicting effects of these two parameters on the residual stresses induced in the substrate have not been reported in the literature.

The present study has been performed to investigate the effect of the spray process parameters including particle impact and gas temperature on the residual stress distribution during the cold spray coating process and to evaluate their role in the evolution of residual stresses in the substrate. Residual stress state has been studied experimentally and numerically considering the peening effect of the impacts as well as the annealing phenomenon as results of the coating temperature and exposure time.

There is a general agreement that grit blasting can increase the deposition efficiency of the coating material by increasing the roughness of the substrate and thus enhancing mechanical anchoring [10–13]; thus grit blasting is frequently used as a preliminary treatment before cold spray coating. Also here all the substrates were grit blasted prior to the coating process.

In this study, the cold spray process has been numerically simulated for different combinations of substrate-coating materials using adopted coating parameters. Several aspects of the process have been implemented in the steps of the numerical simulation. A random distribution has been considered for the particles' diameter, corresponding to the powders used in the experiments; the velocity and temperature of the particles have been calculated individually as a function of their diameter and other process parameters have been approximated through an analytical approach. The residual stress induced through the preliminary grit blasting process has been experimentally measured and considered as initial stress distribution in the substrate model. The preliminary numerical studies show that particle diameter, impact velocity, and temperature have considerable effects on the residual stress induced in the substrate. Then, the effect of annealing on the residual stress is introduced analytically to survey the influence of gas stagnation temperature on the final results. The annealing parameters, presented in Zenner-Wer-Avrami function [14], are derived experimentally by measuring the residual stress in the samples under different exposure coating times and temperatures.

The results of numerical simulation have been verified through experimental in-depth XRD stress measurements. In this regard different combinations of aluminum alloys have been coated and the residual stress on the samples has been experimentally measured and numerically calculated. In order to account for the annealing effect of the process gas temperature in the experimental measurements, a series of grit blasted samples were put through the coating process condition without spraying any powder. The residual stresses were measured on these samples prior to and after the replicated coating process, thus allowing studying the effect of the process temperature solely.

2. Experimental tests

Al5052 and Al6061 aluminum alloys have been considered as substrate materials and coated with Al7075 and pure Al powders. All samples have been grit blasted before coating to provide an increased surface roughness for enhanced mechanical bonding of the coatings to the substrates. The grit blasting parameters are presented in Table 1. The residual stresses have been measured

Table 1
Parameters of grit blasting performed prior to coating.

Pressure	344 kPa (50 psi)
Gas nature	Compressed air
Grit nature	Black alumina
Size	80 Grit
Angle	45°

Table 2
Spray parameters used for the two feedstock powders.

Substrate	Spray parameters	Al7075	Pure Al
Al5052 or Al6061	Pressure (bar)	16	16
	Temperature (°C)	500	350
	Standoff distance (mm)	15	20
	Feeder rotation (rpm)	3	4
	Gas	N_2	N_2
	Traverse velocity (mm/s)	20	100
	Nozzle length (mm)	120	120
	Nozzle throat diameter (mm)	2	2
	Nozzle exit diameter (mm)	6.3	6.3
	Coating time (s)	420	90

using XRD on the grit blasted samples. The samples were then coated using the spray parameters deemed appropriate for powders. Some samples of each series were subjected to the coating process without spraying the powders to study the effect of the process temperature on pre-existent residual stresses induced by grit blasting. By this approach, the state of the stress profile after the replicated coating process (without powder) is solely the effect of the process gas temperature flowing out of the nozzle and the process time.

The use of each of the powders demands different spray parameters, as it is presented in Table 2. The notable difference in the temperatures used for spraying pure Al and Al7075 powders is caused by the fact that spraying pure Al at high temperature results in nozzle clogging, thus a special polymer nozzle has to be used for coating this powder. This nozzle operating temperature is limited to 350 °C, since the polymer cannot withstand higher temperatures [2].

The coating process has been performed at the Ottawa Cold Spray Laboratory (University of Ottawa, Canada) using a commercially available low pressure cold spray system [15] produced by SST Centerline Ltd. (Winsdor, Canada).

To study the residual stress in-depth profile before and after the cold spray process, XRD analysis of the surface layer was performed using an AST X-Stress 3000 diffractometer (radiation CrKα, circular irradiated area of 1 mm diameter, $\sin^2(\psi)$ method, diffraction angle (2θ) of 139° scanned between −45° and 45°). The effective penetration depth of the radiation is approximately 5 μm. Measurements have been carried out in depth step by step by removing a very thin layer of material (0.01/0.02 mm) using an electro-polishing device in order to obtain the in-depth profile of residual stresses and different measurements have been performed in three rotation angles (0°, 45°, and 90°). The particles morphology has been observed by laser diagnostic using a Microtrac S3500 to provide the powder size distribution.

3. The numerical model

A numerical model has been developed to study the peening effect of the particles for two material substrates, Al5052 and Al6061, coated by Al7075. Cold spray coating from the peening point of view is very similar to shot peening process; Bagherifard et al. [16–18] have performed a series of studies on different parameters of the shot peening through verified numerical simulations. The developed model in this paper follows the same approach considering the fact that the process parameters in the latter mentioned shot peening model such as the diameter and the velocity of the shots were ideally considered to be constant and, that the process was carried out at ambient temperature. In the numerical model of cold spray coating the size of the particles should follow a random distribution and, consequently, their velocity and temperature is affected in turn by their size due to the process parameters such as pressure and temperature of the gas. The latter parameters are all considered in the model.

3.1. Particle size and impact position

One of the main challenges to develop a numerical model representing the cold spray process is the correct estimation of the distribution of the particle size and impact position. Fig. 1a shows a SEM image of Al7075 particles used in the current study. The histogram of the powder distribution is obtained using laser diffraction (Fig. 1b).

The Rosin–Rammler model [19,20] is often used to approximate the particle size distribution [21]. This equation is useful for monitoring grinding operations for highly skewed distributions. Li et al. [22] used this distribution for particle size in cold spray coating numerical simulation. Eq. (1) shows the cumulative distribution function (CDF) for modified Rosin–Rammler model [20] which has been fitted to the particles' histogram obtained based on the SEM observations.

$$R(\mathrm{CDF}) = \left\{1 - \exp\left[\frac{\ln(D_p)}{\ln(D_{rr})}^{Q}\right]\right\} \times 100\% \quad (1)$$

In the case of the powder impact positions, although Champagne suggested that the position of the particles on the substrate follows a Gaussian distribution [9], due to the small size of the impact zone, a uniform distribution has been considered for the position of the

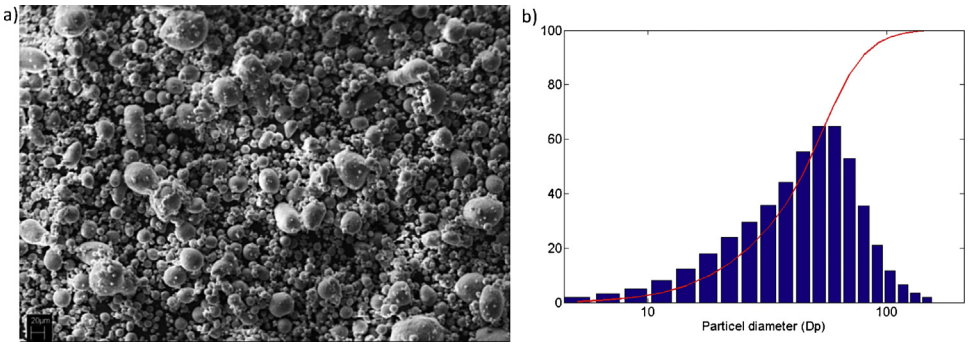

Fig. 1. (a) SEM image Al7075 particles morphology and size distribution (b) histogram and the CDF of the particle size distribution based on Rosin–Rammler (D_{rr} = 45.95; Q = 21.46).

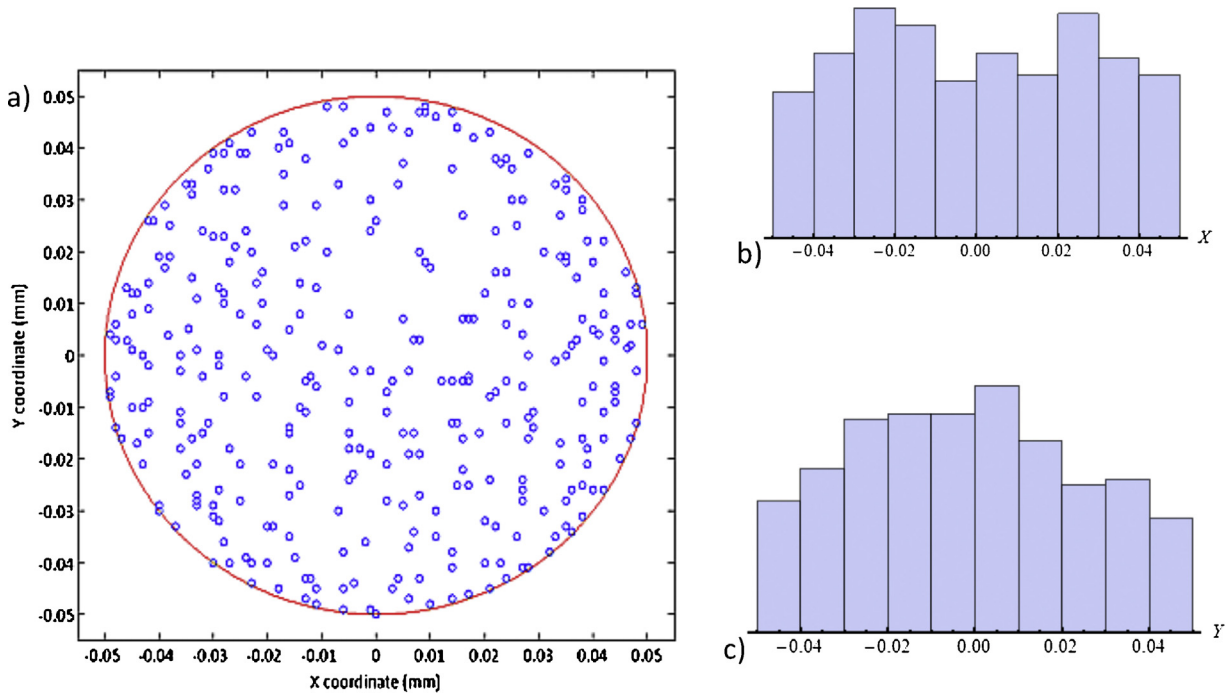

Fig. 2. The center of the particles (blue dots) in one of the models with respect to the borders of the impact zone (red circle). (For interpretation of the references to color in figure legend, the reader is referred to the web version of the article.)

particles in this research. The number of particles in the model has been chosen based on the coating thickness considering the compression ratio of a single impact particle moving at the average velocity of the particles in the process. Fig. 2 shows the positions of the particles center (blue dots) with respect to the impact zone (red circle). The histograms of the particle position in X and Y directions with respect to the impact zone have been illustrated in Fig. 2b and c, respectively. The effect of randomness in the numerical simulation has been studied through repeating the analysis with different parameter combinations.

3.2. Particle velocity

In the coating process, bonding starts when the velocity of the particles exceeds a certain velocity called critical velocity [9,23]. The preliminary studies through single shot impact also revealed that particle velocity is the most important parameter in plastic deformation of the substrate and consequently the induced residual stress. Analytical calculations are used to help estimating the impact velocity. The following formulation presented by Grucijic et al. [24,25] based on the Dykuizen and Smith model [26] has been chosen in order to obtain an estimation of the impact velocity.

$$V_{\text{impact}} = V_p e^{-\rho_{st} * L_{st}/4\rho_p D_p}, \quad \rho_{st} = Re(-1.04 + 2.27\ M - 0.21\,M^2),$$
$$L_{st} = Re(0.97 - 0.02\,M) \tag{2}$$

The Mach number (M) and particle velocity (V_p) at the end of the nozzle can be calculated by Eqs. (3) and (4):

$$M = \left[\kappa_1 \frac{A}{A^*} + (1 - \kappa_1)\right],$$
$$\kappa_1 = 218.0629 - 243.5764\ \gamma + 71.7925\,\gamma^2,$$
$$\kappa_2 = -0.122450 + 0.28130\ \gamma \tag{3}$$

$$\frac{V_p}{V_e} = 0.5\ \left(\frac{V_p}{V_e}\right)_{18} + 0.5\ \left(\frac{V_p}{V_e}\right)_{20}, \qquad \left(\frac{V_p}{V_e}\right)_{20}$$
$$= -e^{\frac{-9\ \mu x}{\rho_p D_p^2 V}} + 1, \qquad \left(\frac{V_p}{V_e}\right)_{18} = -e - \sqrt{\frac{3\ \rho_0 C_D x}{\rho_p D_p}} + 1 \tag{4}$$

The gas velocity at the nozzle exit (V_e) and density of the gas (ρ_0) can be calculated by Eqs. (5) and (6). Gas viscosity (μ) has been evaluated using Sutherland's formula [27,28].

$$\rho_e = \frac{\rho_0}{[1 + ((\gamma - 1)/2)M^2]^{1/\gamma - 1}}, \quad V_e = M\sqrt{\gamma R T_e},$$
$$T_e = \frac{T_0}{[1 + ((\gamma - 1)/2)M^2]}, \quad \rho_0 = \frac{P_0}{RT_0} \tag{5}$$

$$\mu = \mu_0 \left(\frac{a}{b}\right) \left(\frac{T_e}{T_{S0}}\right)^{3/2}, \quad a = 0.555\,T_0 + C; \quad b = 0.555\,T + C \tag{6}$$

3.3. Particle temperature

Papyrin et al. [29] presented an analytical formulation for the particle temperature at the contact surface:

$$T_p = T_0 + C \exp\left(\frac{N_u (6k/d_p^2) x}{\rho_p \vartheta_p C_p}\right)_{|@x=\text{impact dist}},$$

$$N_u = 2a + 0.459\,b\,Re_p^{055}\,Pr^{0.33}, \quad a = \exp(-M)\ \left(1 + \frac{17\,M}{Re}\right)^{-1},$$

$$b = 0.666 + 0.333\ \exp\left(-\frac{17\,M}{Re}\right) \tag{7}$$

where k stands for thermal conductivity, Re_P for the Reynolds number for particles, C_P for the heat capacity of the particles, $Pr = Cp\mu/k$ for the Prandtl number, cp for the specific heat, and μ for the dynamic viscosity measured based on Eq. (7).

Table 3
Mechanical properties of the material [32–34].

Material	Hardness (Rockwell)	Density (kg/m^3)	Specific heat (J/kg K)	Melting point (K)	B_1 (MPa)	B_2 (MPa)	n	C	m
Al 7075-T6	87	2800	960	910	546	674	0.72	0.059	1.56

3.4. Numerical model description

A 3D model developed using commercial finite element code Abaqus/Explicit 6.12-1 [30] is utilized to investigate multiple impact effects. The target is modeled as a rectangular body (0.2 mm × 0.2 mm × 0.25 mm), sufficiently large to avoid the effects of boundary conditions on the residual stress state in the impact area. The impact area of (0.1 mm × 0.1 mm) is located in the center of the rectangular face. Target mesh is set up by C3D8R 8-node linear brick elements with reduced integration and hourglass control. The bottom side face of target is meshed by the so-called half infinite elements that provide quiet boundaries by minimizing the reflection of dilatational and shear waves back in to the region of interest [30].

The material model plays an important role in the results and the behavior of the substrate/particle. In this study combined isotropic kinematic hardening model [31] has been chosen for the substrate and the Johnson-Cook model [32] presented in Eq. (8) has been used for the powders; the material constants are presented in Table 3.

$$\sigma_{eq} = [B_1 + B_2(\in_p)^n]\left[1 + C\ln\left(\frac{\dot{\in}_p}{\dot{\in}_{p0}}\right)\right] \times \left[1 - \left(\frac{T - T_{init}}{T_{melt} - T_{init}}\right)^m\right] \tag{8}$$

Fig. 3(a and b) shows different views of the model developed in Abaqus. In this figure, the arrangement and the particle size distribution have been presented with respect to the red circle which represents the impact zone. The in-depth stress measured experimentally on the grit-blasted samples before coating process has been considered as predefined stress field in the FE model before the particles impact. The numerical model has been developed for Al7075 powders on both Al5052 and Al6061 as the substrate. A model that considers random particle impact position, random impact sequence as well as random diameter of the particles, and calculates the velocity and temperature depending on process parameters has been developed using a home-made Python [35] subroutine.

3.5. Analytical study of annealing effect

If a pure metal is annealed for several hours at a temperature that is half of its melting point and then cooled slowly to room temperature, almost total relaxation of the residual stresses from any previous mechanical and chemical treatment can be achieved [1]. The necessary annealing time depends essentially on the work piece dimensions and the material state. The effect of time on residual stress relaxation can be linearized with the help of the Zenner-Wert-Avrami function [14]:

$$\frac{\sigma^{rs}}{\sigma_0^{rs}} = \exp[-(St_a)^m] \tag{9}$$

where m is a numerical term dependent on the dominant relaxation mechanism and S is a function dependent on material and temperature according to:

$$S = S_1 \exp\left(\frac{-\Delta H}{kT_a}\right) \tag{10}$$

where S_1 is a constant. It follows from Eq. (9) that:

$$\log\left(\ln\left(\frac{\sigma_0^{rs}}{\sigma^{rs}}\right)\right) = m\log t_a + m\log S \tag{11}$$

Eq. (11) shows the linear behavior between annealing time and relieved stress at the same temperature; i.e. having the constant in this equation it is possible to estimate the relieved stress in different annealing times and the same temperature.

Based on Eqs. (9) and (11), in samples with equal geometry, volume, and material, if annealing parameters including time and temperature are the same, the fraction of $\sigma_0^{rs}/\sigma^{rs}$ will remain constant. Therefore, by gathering the information of the as-coated samples (gone through coating process without powders), it is possible to apply the annealing effect on numerical simulations' results to evaluate the final distribution of residual stresses.

4. Results and discussion

The residual stress measured in as-coated and grit blasted samples in both Al5052 and Al6061are shown in Fig. 4. The results of

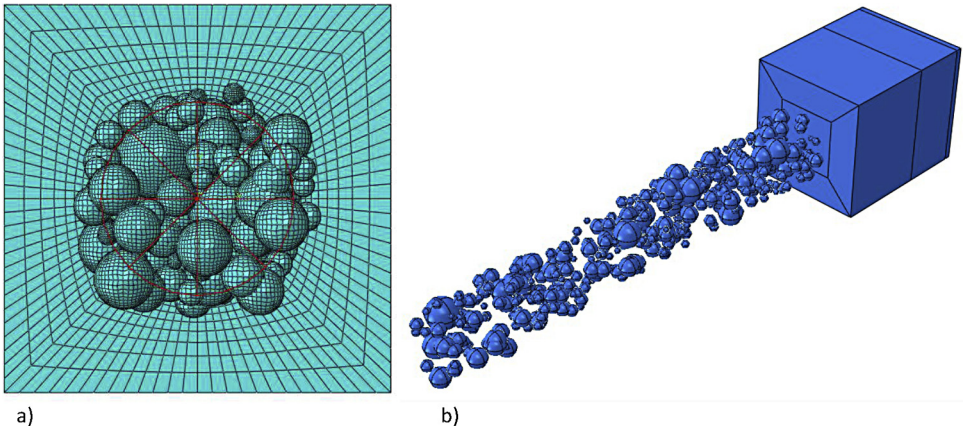

Fig. 3. (a) Top and (b) isometric view of one of the models developed for residual stress calculations (the red area represents the "impact-zone"). (For interpretation of the references to color in figure legend, the reader is referred to the web version of the article.)

Table 4
Calculation of annealing constant at each depth for Al5052.

	Experimental measurement			Numerical estimation	
Depth	Grit blasted	Coated as Al7075	$\sigma_0^{rs}/\sigma^{rs}$	Numerical results	Annealing the results
0	−79.79	−18.35	4.35	−35.31	−8.12
50	−118.03	−47.63	2.48	−109.133	−44.00
100	−122.64	−51.98	2.36	−109.6	−46.44
150	−114.82	−46.82	2.45	−43.08	−17.58

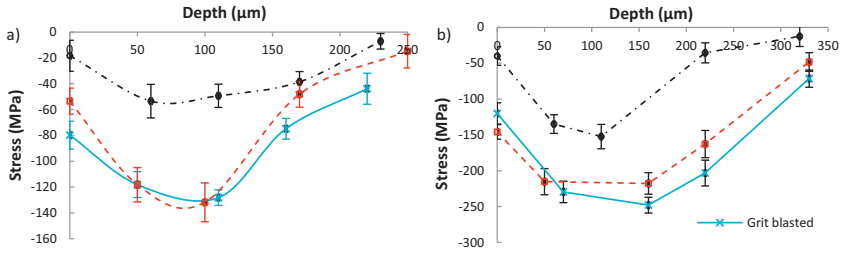

Fig. 4. The effect of coating temperature on relieving the residual stress in the samples (a) Al5052 and (b) Al6061.

this preliminary study show the effect of coating time and temperature on relieving the residual stress of the grit blasted samples that can be a lead to derive Zenner-Wert-Avrami parameters.

Considering that no powder has been used in the as-coating process, the alterations of residual stresses are attributed solely to the process time and temperature. In Fig. 4(a) and (b), the solid lines show the average residual stress measured in grit blasted samples, the dashed line shows the samples as-coated with the spray parameters used for spraying pure Al, and the dashed dot style line shows the samples as-coated with the spray parameters used for spraying Al7075. The graphs, for both Al6061 and Al5052 substrates, show a considerable effect of the coating temperature and spray time on relieving the residual stress in the samples. The shorter coating time and lower spray temperature result in less annealing effect as was expected; i.e. in the case of the spray parameters used to spray pure Al powders where the temperature is lower and the coating time is shorter than for the case of Al7075 powder, thus the stresses are less relieved. In both substrates, Al5052 and Al6061, a substantial decrease is observed after spraying using the spray parameters used to spray Al7075. However, the samples sprayed by the parameters used to spray pure Al do not show a considerable change in the residual stress profile; this can be attributed to the different process parameters. As reported in Table 2, Al7075 is sprayed using higher temperature and notably longer process duration. By assuming the isothermal process condition and considering Zenner-Wert-Avrami approach, the value of $\sigma^{rs}/\sigma_0^{rs}$ in Eq. (9) can be derived at each depth. Considering the constant time and temperature, the ratio of residual stresses before and after annealing would be the same as that for the coated samples; these values, obtained from experimental XRD measurements, have been used in order to modify the numerical results after the impact at each depth. The results and the steps of the calculation in some depths are presented in Table 4. It has to be mentioned that the solid line in Fig. 4(a) and (b), which corresponds to the residual stresses induced by grit blasting, has been considered in numerical models for both materials as pre-stress.

Fig. 5 shows the comparison of the residual stress measured for the coated Al5052 (Fig. 5a) and Al6061 (Fig. 5b) substrates. The y-axis is the interface and the positive x values in depth in Fig. 5 represent measurements in the substrate with negative part showing the measurement related to deposited material. The black lines show the results for the samples coated with Al7075 and red lines show the results for the samples coated with pure aluminum. The dashed lines in both red and black lines show the range of the measurement at different angles of the stress XRD results. In both materials, Al5052 and Al6061, samples coated with pure Al have the higher residual stress in the substrate with respect to the ones coated with Al7052; although it is not shown in the graph, the maximum value measured for the Al6061 coated with pure Al is about 300 MPa with respect to 250 MPa in the case of Al7075. This

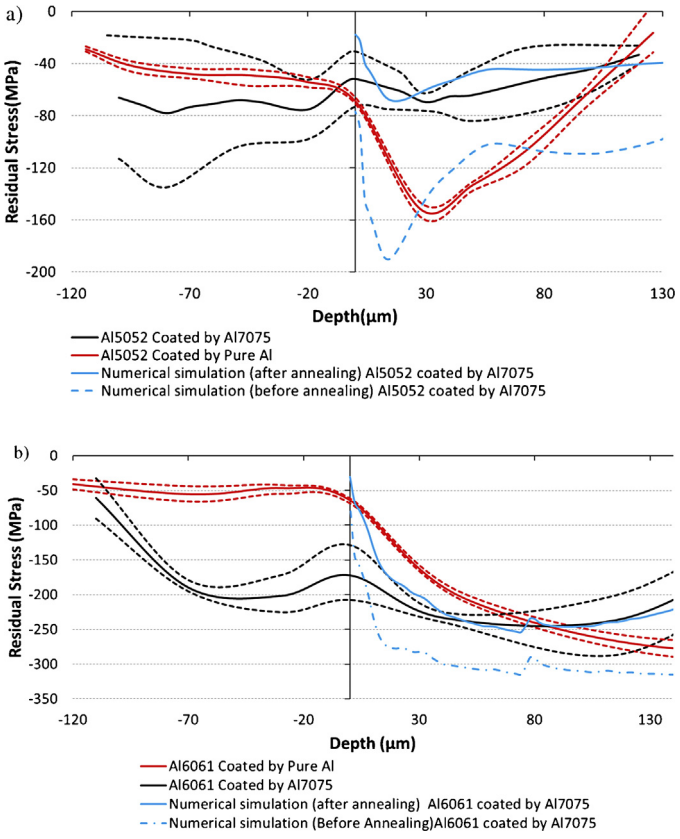

Fig. 5. Residual stress measurement for the coated samples with Al7075 and pure Al compared to the numerical simulation (a) Al5052 (b) Al6061 (red and black dashed lines represent the range of the measurement at different angles). (For interpretation of the references to color in figure legend, the reader is referred to the web version of the article.)

is attributed to the coating time and temperature which relieve the residual stress in the samples. It can be postulated that although the velocity of the particles in both Al7075 and Pure Al coating is the same and even Al7075 is harder than Pure Al, higher temperature in Pure Al coating and annealing effect as the results of the process temperature can relief the stress induced by powders in the coated samples and result in lower residual stress in Al7075 compared to pure Al.

The measurements in samples coated with Al7075 in both Al5052 and Al6061 substrates show broader dispersion at different angels of diffraction with respect to samples coated by Pure Al.

The results of numerical simulation are added to the same graph in order to make a comparison between numerical simulations and experimental analyzes; where the blue lines show the results obtained from the simulation before annealing (dashed blue line) and after annealing (solid blue line). The same annealing parameters obtained from as-coated sample test were used in order to apply the effect of annealing on the samples with respect to time and temperature of the coating. As it is observed in Fig. 5, the numerical results are in good agreement with experimental measurements, lying within experimental results range except for the results just at the surface of the substrate. The graph shows the great contribution of the annealing in relieving the stress in the substrate after applying the exact same parameters obtained from the experiment; the maximum stress in Al5052 is relieved from about 180 MPa to less than 80 MPa and in the case of Al6061 from 300 MPa to 250 MPa. It is interesting to mention that the difference in the maximum stress in numerical simulation before and after annealing has almost the same magnitude as the maximum values between samples coated by pure Al and Al7075. The dissimilarity of the results just on the substrate surface can be mostly attributed to the fact that the bonding phenomenon is not considered in the simulation; i.e. the bonding of the particles to the substrate has an apparent effect on the state of the stress right on the surface. However, below the surface the FE model is able to predict the stress profile with good approximation.

5. Conclusions

The evolution of residual stress in cold spray coating process has been studied through numerical and experimental analysis. On the basis of the results the following conclusions are drawn:

1. In the cold spray coating process, constant bombarding of particles induces residual stresses in the substrate. Although the process gas temperature is less than the melting point of the materials involved, it was postulated to have negative annealing effect on the favorable compressive residual stress induced by previous grit blasting and the particles impact. This effect was clearly noted by means of experiments on samples formerly grit blasted and then submitted to the cold spray process without using powders. The results of the experimental measurements show the considerable effect of the process temperature on promoting residual stress relaxation.
2. A two-steps approach aimed at realistically simulating the cold spray process was developed to obtain the final residual stress state in the substrate. It considers the residual stresses induced by grit blasting, particle size distribution, random impact position, and the corresponding velocity and temperature for the particles as a function of their size. The first step is based on a FE\Explicit simulation and considers different material models compatible with the phenomenon. Even if some approximation is considered with respect to the real process (the bonding of the particles on the substrate is not modeled) the numerical model allows for studying the peening effect of the particles. The results obtained from the FE simulation do not consider the effect of the annealing. In this regard, in the second analytical step the Zenner-Wert-Avrami method has been utilized to apply the annealing effect on the numerical results using the experimental measurements performed on not coated samples.
3. The ability of the numerical approach to correctly estimate the final residual stresses induced by cold spray are verified by means of XRD experimental measurements. The comparison of the residual stress in-depth profile shows a satisfactory agreement with experimental data, except for the stresses on the substrate surface. This was interpreted as the effect of the bonding phenomenon of the particles to the substrate, which is not considered in the numerical model.
4. The current study also indicates that a longer coating time and higher process temperature plays an important role on relieving the residual stress in the samples; i.e. the lesser coating time of the components is, the lesser the residual stress induced by the process is relieved and the same is true for the process temperature.

References

[1] G. Totten, M. Howes, T. Inoue, Handbook of Residual Stress and Deformation of Steel, ASM International, Materials Park, OH, 2002, pp. 118–120.
[2] R. Ghelichi, D. MacDonald, S. Bagherifard, H. Jahed, M. Guagliano, B. Jodoin, Microstructure and fatigue behavior of cold spray coated Al5052, Acta Materialia 60 (2012) 6555–6561.
[3] K. Taylor, B. Jodoin, J. Karov, P. Richer, Particle loading effect in cold spray, in: Proceeding of the International Thermal Spray Conference, May 2–4, Basel Switzerland, 2005.
[4] R.C. McCune, W.T. Donlon, O.O. Popoola, E.L. Cartwright, Characterization of copper layers produced by cold gas-dynamic spraying, Journal of Thermal Spray Technology 9 (2000) 73–82.
[5] S. Bagherifard, I.F. Pariente, R. Ghelichi, M. Guagliano, S. Vezzù, Effect of shot peening on residual stresses and surface work-hardening in cold sprayed coatings, vol. 417, Key Engineering Materials, Durnten-Zurich, 2010, pp. 397–400.
[6] V. Luzin, K. Spencer, M.X. Zhang, Residual stress and thermo-mechanical properties of cold spray metal coatings, Acta Materialia 59 (2011) 1259–1270.
[7] Y.C. Tsui, T.W. Clyne, Thin Solid Films 306 (1997) 23.
[8] K. Spencer, V. Luzin, N. Matthews, M.X. Zhang, Residual stresses in cold spray Al coatings: the effect of alloying and of process parameters, Surface & Coatings Technology 206 (2012) 4249–4255.
[9] V.K. Champagne, The Cold Spray Materials Deposition Process, Fundamentals and Applications, Woodhead Publishing, Cambridge, 2007.
[10] T.S. Price, P.H. Shipway, D.G. McCartney, Effect of cold spray deposition of a titanium coating on fatigue behavior of a titanium alloy, Journal of Thermal Spray Technology 15 (2006) 507–512.
[11] X.J. Ning, J.H. Jang, H.J. Kim, C.J. Li, C. Lee, Cold spraying of AlSn binary alloy: coating characteristics and particle bonding features, Surface & Coatings Technology 202 (2008) 1681–1687.
[12] D.E. Wolfe, T.J. Eden, J.K. Potter, A.P. Jaroh, Investigation and characterization of Cr_3C_2 based wear-resistant coatings applied by the cold spray process, Journal of Thermal Spray Technology 15 (2006) 400–412.
[13] L. Legoux, E. Irissou, C. Moreau, Effect of substrate temperature on the formation mechanism of cold sprayed aluminum, zinc, and tin coating, Journal of Thermal Spray Technology 16 (2007) 619–627.
[14] M.W. Fine, Introduction to Phase Transformations in Condensed Systems, Macmillan, New York, 1965.
[15] R. Maev, V. Leshchynsky, Introduction to Low Pressure Gas Dynamic Spray, Wiley-VCH Verlag GmbH & Co. KGaA, Weinheim, 2008.
[16] S. Bagherifard, R. Ghelichi, M. Guagliano, Numerical and experimental analysis of surface roughness generated by shot peening, Applied Surface Science 258 (July 18) (2012) 6831–6840.
[17] S. Bagherifard, R. Ghelichi, M. Guagliano, On the shot peening surface coverage and its assessment by means of finite element simulation: a critical review and some original developments, Applied Surface Science 259 (2012) 186–194.
[18] S. Bagherifard, R. Ghelichi, M. Guagliano, A numerical model of severe shot peening (SSP) to predict the generation of a nanostructured surface layer of material, Surface and Coatings Technology 204 (September 24) (2010) 4081–4090.
[19] K.N. Ramakrishnan, Modified rosin rammler equation for describing particle size distribution of milled powders, Journal of Materials Science letters 19 (2000) 1903–1906.
[20] P. Rosin, E. Rammler, The laws governing the fineness of powdered coal, Journal of the Institute of Fuel 7 (1933) 29–36.
[21] T. Allen, Powder sampling and particle size determination, Elsevier, USA, 2003.

[22] C.J. Li, W.Y. Li, H. Liao, Examination of the critical velocity for deposition of particles in cold spraying, Journal of Thermal Spray Technology 15 (2006) 212–222.
[23] T. Schmidt, F. Gärtner, H. Assadi, H. Kreye, Development of a generalized parameter window for cold spray deposition, Acta Materialia 54 (February 3) (2006) 729–742.
[24] R. Ghelichi, S. Bagherifard, M. Guagliano, M. Verani, Numerical simulation of cold spray coating, Surface and Coatings Technology 205 (September 23–24) (2011) 5294–5301.
[25] M. Grujicic, C.L. Zhaoa, C. Tonga, W.S. DeRosset, D. Helfritch, Analysis of the impact velocity of powder particles in the cold-gas dynamic-spray process, Materials Science and Engineering 368 (2004) 222–230.
[26] M. Grujicic, W.S. DeRosset, D. Helfritch, Flow analysis and nozzle-shape optimization for the cold-gas dynamic-spray process, Journal of Engineering Manufacture 217 (2003) 1–11.
[27] R.C. Dykhuizen, M.F. Smith, Gas dynamic principles of cold spray, Journal of Thermal Spray Technology 7 (1998) 205–212.
[28] C. Robert (Ed.), CRC Handbook of Chemistry and Physics, CRC Press, Boca Raton, 1984.
[29] A. Papyrin, V. Kosarev, S. Klinkov, A. Alkhimov, V. Fomin, Cold Spray Technology, Elsevier, Oxford, 2006.
[30] Abaqus 6.12-1, Analysis User's Manual, Simulia, 2012.
[31] J. Lemaitre, J.L. Chaboche, Mechanics of Solid Materials, Cambridge University Press, Cambridge, 1994.
[32] G.R. Johnson, W.H. Cook, A constitutive model and data for metals subjected to large strain, high strain rates and high temperature, in: Proceedings of the 7th International Symposium on Ballis-tics, vol. 4, 1983, pp. 541–547.
[33] N. Brar, V. Joshi, B. Harris, Constitutive model constants for Al7075-T651 and Al7075-T6, in Constitutive Model Constants for Al7075-T651 and Al7075-T6, 2009.
[34] http://asm.matweb.com/search/SpecificMaterial.asp?bassnum=MA7075T6
[35] Python documentation, http://docs.python.org/